

## Current transient spectroscopy for trapping analysis on Au-free AlGaIn/GaN Schottky barrier diode

J. Hu, S. Stoffels, S. Lenci, B. Bakeroot, R. Venegas, G. Groeseneken, and S. Decoutere

Citation: [Applied Physics Letters](#) **106**, 083502 (2015); doi: 10.1063/1.4913575

View online: <http://dx.doi.org/10.1063/1.4913575>

View Table of Contents: <http://scitation.aip.org/content/aip/journal/apl/106/8?ver=pdfcov>

Published by the [AIP Publishing](#)

---

A banner for the Applied Physics Letters journal. It features the AIP logo and the text 'Applied Physics Letters' at the top. Below this, it says 'Meet The New Deputy Editors'. At the bottom, there are three circular portraits of the new deputy editors: Alexander A. Balandin, Qing Hu, and David L. Price.

**AIP | Applied Physics Letters**

**Meet The New Deputy Editors**

 Alexander A. Balandin

 Qing Hu

 David L. Price

# Current transient spectroscopy for trapping analysis on Au-free AlGaN/GaN Schottky barrier diode

J. Hu (胡杰),<sup>1,2,a)</sup> S. Stoffels,<sup>2</sup> S. Lenci,<sup>2</sup> B. Bakeroot,<sup>2,3</sup> R. Venegas,<sup>2</sup> G. Groeseneken,<sup>1,2</sup> and S. Decoutere<sup>2</sup>

<sup>1</sup>Department of Electrical Engineering (ESAT), KU Leuven, 3001 Leuven, Belgium

<sup>2</sup>imec, Kapeldreef 75, 3001 Leuven, Belgium

<sup>3</sup>Centre for Microsystems Technology (CMST), imec and Ghent University, Technologiepark 914a, 9052 Gent, Belgium

(Received 19 December 2014; accepted 13 February 2015; published online 24 February 2015)

This paper presents a combined technique of high voltage off-state stress and current transient measurements to investigate the trapping/de-trapping characteristics of Au-free AlGaN/GaN Schottky barrier diodes. The device features a symmetric three-terminal structure with a central anode contact surrounded by two separate cathodes. Under the diode off-state stress conditions, the two separate cathodes were electrically shorted. The de-trapping dynamics was studied by monitoring the recovery of the two-dimensional electron gas (2DEG) current at different temperatures by applying 0.5 V at cathode 2 while grounding cathode 1. During the recovery, the anode contact acts as a sensor of changes in diode leakage current. This leakage variation was found to be mainly due to the barrier height variation. With this method, the energy level and capture cross section of different traps in the AlGaN/GaN Schottky barrier diode can be extracted. Furthermore, the physical location of different trapping phenomena is indicated by studying the variation of the diode leakage current during the recovery. We have identified two distinct trapping mechanisms: (i) electron trapping at the AlGaN surface in the vicinity of the Schottky contact which results in the leakage reduction (barrier height  $\phi_B$  increase) together with  $R_{ON}$  degradation; (ii) the electron trapping in the GaN channel layer which partially depletes the 2DEG. The physical origin of the two different traps is discussed in the text. © 2015 AIP Publishing LLC. [<http://dx.doi.org/10.1063/1.4913575>]

Over the last few years, gallium nitride (GaN)-based electronic devices have been considered as promising candidates over silicon devices for future generations of high-power and high-frequency applications.<sup>1,2</sup> One of the prominent features of GaN-based devices such as high electron mobility transistors (HEMTs) and heterogeneous Schottky barrier diodes (SBDs) is the formation of two-dimensional electron gas (2DEG) at the AlGaN/GaN heterointerface due to the spontaneous and piezoelectric polarization without intentional doping.<sup>3,4</sup> However, the stability of the device performance is affected by trapping mechanisms occurring at the AlGaN surface,<sup>5,6</sup> at the gate dielectric/AlGaN interface,<sup>7</sup> in the AlGaN barrier,<sup>8</sup> or in the buffer,<sup>9–11</sup> thus degrading the superior properties of 2DEG channel. Several researchers have performed the study of trapping effects in AlGaN/GaN transistors by combined pulsed and  $R_{ON}$  transient measurements. Joh and del Alamo have presented a current-transient methodology to study the electron trapping in GaN HEMTs.<sup>8</sup> Liao *et al.* and Bisi *et al.* have reported the back-side virtual gate effects in AlGaN/GaN HEMTs due to the electron trapping in the AlGaN back-barrier.<sup>10,11</sup> Meneghini *et al.* have investigated the trapping mechanisms in GaN HEMTs by understanding the role of bias conditions in electron trapping.<sup>12</sup>

The aim of this paper is to present a combined off-state stress and current transient measurements to investigate the trapping mechanisms in lateral AlGaN/GaN SBDs. Differently from common two-terminal AlGaN/GaN SBDs

reported in literature,<sup>13,14</sup> the device in this study features a three-terminal structure with two separate cathodes surrounding a central anode contact. Temperature-dependent transient measurements on 2DEG (from 25 °C to 135 °C) have been carried out to extract the activation energy and capture cross section of related traps. Moreover, the variation of the diode leakage current during recovery is analyzed to identify the physical location of trapping phenomena.

The AlGaN/GaN epitaxial layers were grown on 8-in. GaN-on-Si wafers by using metal organic chemical vapor deposition (MOCVD) tool. The epi-structure consists of 3 nm GaN capping layer, 10 nm  $\text{Al}_{0.25}\text{Ga}_{0.75}\text{N}$  barrier, a 150 nm GaN channel layer, a stack of buffer layers (400 nm  $\text{Al}_{0.74}\text{Ga}_{0.26}\text{N}$ /400 nm  $\text{Al}_{0.44}\text{Ga}_{0.56}\text{N}$ /1800 nm  $\text{Al}_{0.21}\text{Ga}_{0.79}\text{N}$ ), and a 200 nm AlN nucleation layer on *p*-type Si(111) substrate. The surface of the epi-stack has been passivated by 140 nm  $\text{Si}_3\text{N}_4$  layer deposited at 750 °C by means of rapid thermal chemical vapor deposition (RTCVD). The removal of the  $\text{Si}_3\text{N}_4$  passivation layer was performed by  $\text{SF}_6$  dry etching at the anode region. A  $\text{N}_2$  plasma cleaning treatment of the AlGaN surface was given to remove the traps before the deposition of the anode metal.<sup>15</sup> A Au-free metal stack for the anode consists of 20 nm TiN/20 nm Ti/250 nm Al/20 nm Ti/60 nm TiN. A metal stack of 5 nm Ti/100 nm Al/20 nm Ti/60 nm TiN was deposited for the cathode contact formation, which was annealed at 550 °C.<sup>16</sup> A schematic of the AlGaN/GaN SBD studied in the work is shown in Fig. 1(a) with two cathodes (C1 and C2). The Schottky contact length ( $L_{SC}$ ), the anode finger width, and the anode-cathode distance ( $L_{AC}$ ) were 9  $\mu\text{m}$ , 100  $\mu\text{m}$ , and 5  $\mu\text{m}$ , respectively.

<sup>a)</sup>Electronic mail: Jie.Hu@imec.be

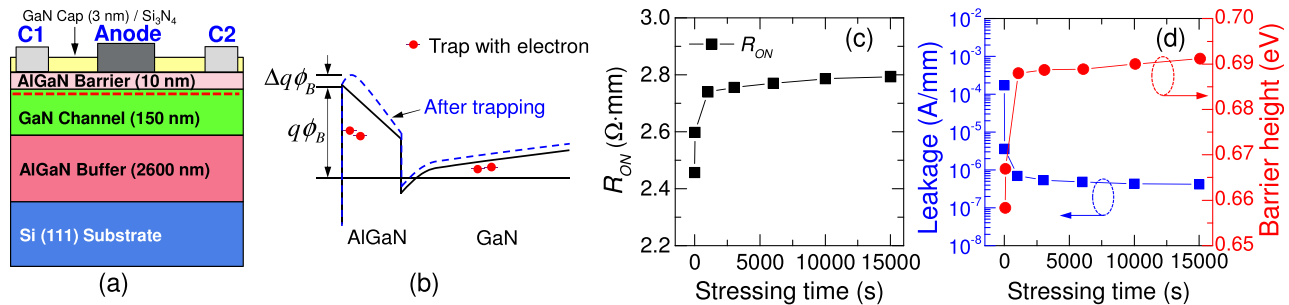


FIG. 1. (a) The schematic cross-section of the AlGaIn/GaN Schottky barrier diode. (b) Conduction band profile of the AlGaIn/GaN heterostructure before (solid line) and after off-state stress (dashed line). (c) The  $R_{ON}$  degradation of the SBD during off-state stress. (d) The leakage current (left axis) and extracted Schottky barrier height (right axis) of the SBD during off-state stress.

In a typical power application with GaN-based technology, e.g., a DC/DC converter, the AlGaIn/GaN SBD is switched passively from off-state (where diode reverse voltage  $V_R$  has a high negative value) to on-state (where the diode forward voltage  $V_F$  has a low positive value). During the off-state operation, the SBD is subjected to a high electric field condition, which gives rise to electron injection and trapping phenomena at the AlGaIn surface (at the corner of the Schottky contact) or in the GaN channel and AlGaIn buffer layers.<sup>17</sup>

As shown in Fig. 1(b), the conduction band will be lifted up due to the trapped electrons (in the AlGaIn barrier and in the GaN channel layer) resulting in a lower 2DEG density compared with the fresh condition.<sup>18</sup> This reduction in 2DEG density directly reflects on the increase of the diode on-resistance (in Fig. 1(c)) after constant voltage ( $V_R$  of  $-100$  V) off-state stress measurement. Furthermore, the leakage current of the stressed SBD showed two to three orders of magnitude reduction after  $\sim 4$  h of stressing, as is depicted in Fig. 1(d). The significant changes in leakage of the stressed device are correlated with the increase of the effective Schottky barrier height (SBH)  $\phi_B$  (in Fig. 1(d) to the right axis) which was extracted from the forward characteristics based on the thermionic emission model. The trapped region at the AlGaIn surface in the vicinity of the Schottky contact forms a virtual gate effect and shows a local increase of the surface potential.<sup>18</sup> The modified potential barrier results in a lower tunneling probability and a lower leakage current for the diode.<sup>19</sup> The filling of the traps located in the GaN channel or AlGaIn buffer layers (in the

access region) will only contribute to the  $R_{ON}$  increase rather than affecting the SBH  $\phi_B$  directly.

To identify the related traps (activation energy, capture cross section, and physical location) in AlGaIn/GaN SBD, we developed a current-based methodology which consists of an off-state stress stage and a current recovery stage shown in Fig. 2(a). The measurements were performed by using a Semiconductor Device Analyzer (Agilent B1500A). During the stress, the device was biased in the off-state for 10 s to fill the traps. The stress voltage ( $V_R$  of  $-100$  V) was applied at the anode, and cathode 1 and cathode 2 were grounded. During the recovery, the anode and cathode 1 contacts were grounded while 0.5 V was applied on the cathode 2. After the removal of the stress voltage at the anode, the 2DEG was replenished partially due to the combined effect of net positive polarization charges at the AlGaIn/GaN interface and the trapped electrons.<sup>5,18</sup> In the recovery stage, we monitor the recovery of the current flowing through the 2DEG instead of the diode forward current (in the on-state). It needs to be noted that the voltage between anode and cathode 2 is  $-0.5$  V, in this case there is a leakage current flowing through the anode contact at its perimeter.<sup>19</sup> The variation of the leakage current during recovery was analyzed to identify the location of related traps. Whenever there is a de-trapping of electrons at the AlGaIn surface, the effective barrier height  $\phi_B$  reduces and the diode leakage current can show an increase accordingly. The recovery measurements were carried out at temperatures ranging from  $25^\circ\text{C}$  to  $135^\circ\text{C}$  with a predefined recovery time of 3500 s. The recovery current (through cathode 2) and the diode

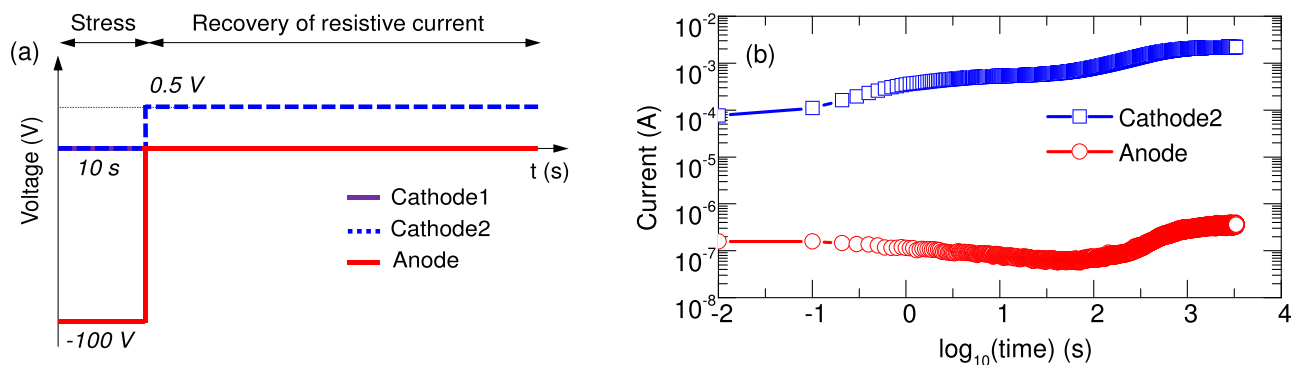


FIG. 2. (a) The combined measurement procedure developed in this study. The device is biased in the off-state ( $V_R = -100$  V) for 10 s to fill certain traps followed by a recovery of the 2DEG resistive current. (b) The current monitored through cathode 2 and anode during the recovery. The recovery of the 2DEG resistor (through cathode 2) is used for the trap analysis, and the current through the anode is the diode leakage current at  $V_R$  of  $-0.5$  V.

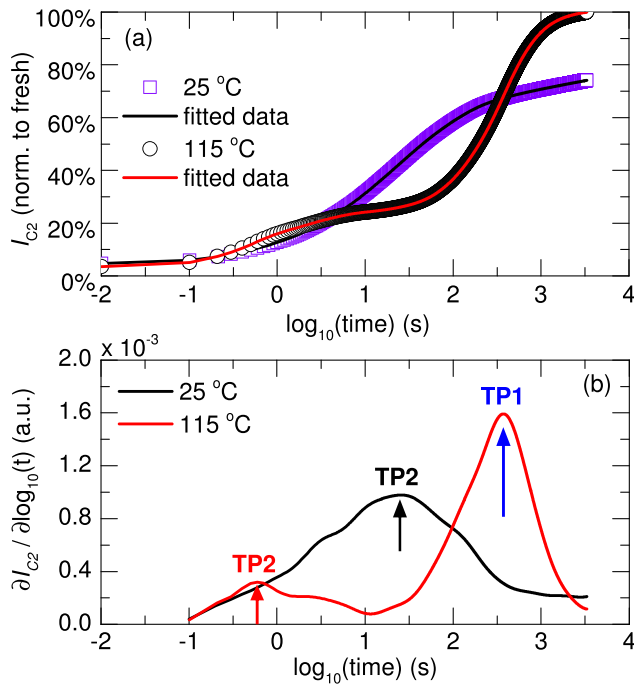


FIG. 3. (a) The normalized recovery current measurement at 25 °C and 115 °C. (b) The time-constant spectra (derivative of the current transients) evaluated at 25 °C and 115 °C.

leakage current (at  $V_R$  of  $-0.5$  V) are shown in Fig. 2(b). The 2DEG resistive current is shown to be more than three orders of magnitude higher than the leakage current, and we use the resistive current for the extrapolation of traps.<sup>8</sup>

To extract the activation energy of traps, the de-trapping resistive current  $I_{C2}$  was first fitted by a least-mean-square approach with a sum of 400 exponentials and equally spaced time constants logarithmically ranging from 0.01 s to 10 000 s.<sup>8</sup> In Fig. 3(a), the raw data and fitted curve of the recovery currents at 25 °C and 115 °C are shown. The current has been normalized to the value obtained from the fresh device at 25 °C and 115 °C, respectively. At room temperature, the device has recovered 74.13% of its current after recovery time of 3500 s. To have a full recovery of the current, the device requires longer time than 3500 s at 25 °C or the recovery at much higher temperature (i.e., at 115 °C) with predefined recovery time. From the time-constant spectra (in Fig. 3(b)) at 115 °C, two distinct time constants were observed, which

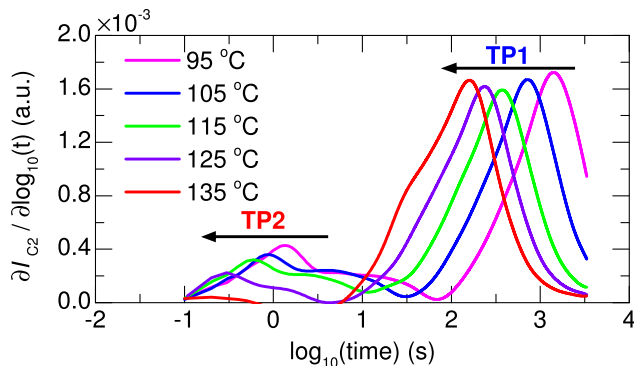


FIG. 4. The time-constant spectra evaluated from 95 °C to 135 °C showing the de-trapping kinetics of TP1 and TP2.

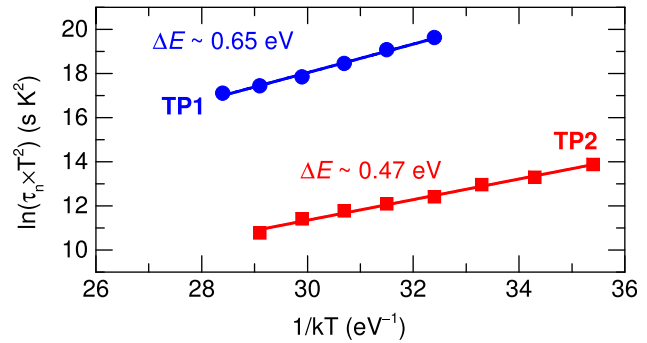


FIG. 5. Arrhenius plot of the time constant spectra for TP1 and TP2.

are labeled as TP1 ( $\tau \sim 373.6$  s) and TP2 ( $\tau \sim 0.6$  s). At room temperature, there is only one time constant ( $\tau \sim 25.7$  s) shown which corresponds to the de-trapping of TP2.

The time-constant spectra for de-trapping transients of TP1 and TP2 are shown in Fig. 4 evaluated from 95 °C to 135 °C. With these temperature-dependent measurements, the activation energy and capture cross section of TP1 and TP2 can be extrapolated based on the equation<sup>20</sup> below

$$\ln(\tau_n \times T^2) = (E_C - E_T) \frac{1}{kT} - \ln(\sigma_n \times \gamma_n). \quad (1)$$

The Arrhenius plot (shown in Fig. 5) indicates that TP1 has an activation energy of 0.65 eV and a cross section of  $0.89 \times 10^{-20} \text{ cm}^{-2}$ , while TP2 has an activation energy of 0.47 eV and a cross section of  $2.85 \times 10^{-20} \text{ cm}^{-2}$ .

To identify the physical location of these two trapping/de-trapping phenomena, we have analyzed the leakage current through the anode during the recovery transient at different temperatures. The leakage current is exponentially dependent on the SBH  $\phi_B$  (at fixed voltage). As is shown in Fig. 6, the leakage current shows a slight reduction in the logarithmic time window from  $-2$  to  $1.5$  followed by an increase of the leakage in the time window (in logarithmic scale) from  $2$  to  $3.5$ . By comparing Fig. 6 with the time-constant spectra of Fig. 4, we notice that the leakage current showed the reduction during the de-trapping of TP2 and the increase during the de-trapping of TP1. As the de-trapping occurs (for both TP1 and TP2), the 2DEG resistance and potential will be changed. The reduction in leakage may be due to the variation of the voltage drop across the diode (at its perimeter) during the de-trapping of the TP2 in the GaN

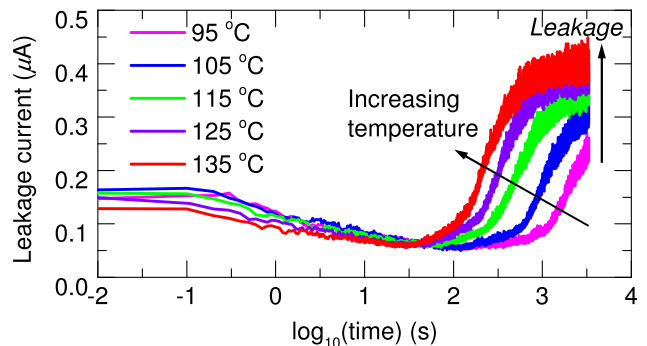


FIG. 6. The SBD leakage during the recovery monitored from 95 °C to 135 °C.

channel layer. When the de-trapping process occurs at the AlGa<sub>N</sub> barrier surface (at the corner of the Schottky contact), the effective SBH is reduced with an increase of the leakage current (as the opposite phenomenon in Fig. 1(d)). The leakage increase in Fig. 6 identifies TP1 as a surface trap. Okino *et al.*<sup>21</sup> have reported the surface traps of 0.62 eV and 0.68 eV for AlGa<sub>N</sub>/Ga<sub>N</sub> MIS-HEMTs and AlGa<sub>N</sub>/Ga<sub>N</sub> HEMTs, these values are very close to the one extracted from our work. However, to know the microscopic nature of this surface trap is still challenging. The origin of TP2 ( $E_A = 0.47$  eV) may be related to the C/O/H impurities in the Ga<sub>N</sub> layer,<sup>22,23</sup> which were introduced unintentionally during the growth of the epitaxial layers.

In conclusion, we report here a current-based transient spectroscopy on Au-free AlGa<sub>N</sub>/Ga<sub>N</sub> SBD to investigate the trapping mechanisms during the diode off-state stress. Two distinct trap levels have been extrapolated from this method. Furthermore, the diode leakage current showed different characteristics during the de-trapping of TP1 and TP2. The trapping at the AlGa<sub>N</sub> surface (TP1) and in the Ga<sub>N</sub> channel layer (TP2) results in the reduction of 2DEG density and increase of the  $R_{ON}$  for the diode. The filling of the surface traps (TP1) at the corner of the Schottky contact causes the leakage reduction and barrier height increase.

<sup>1</sup>O. Aktas, Z. Fan, S. Mohammad, A. Botchkarev, and H. Morkoc, *Appl. Phys. Lett.* **69**, 3872 (1996).

<sup>2</sup>Y. Cao, K. A. Wang, A. Orlov, H. Xing, and D. Jena, *Appl. Phys. Lett.* **92**, 152112 (2008).

<sup>3</sup>O. Ambacher, J. Smart, J. Shealy, N. Weimann, K. Chu, M. Murphy, W. Schaff, L. Eastman, R. Dimitrov, L. Wittmer *et al.*, *J. Appl. Phys.* **85**, 3222 (1999).

<sup>4</sup>O. Ambacher, B. Foutz, J. Smart, J. Shealy, N. Weimann, K. Chu, M. Murphy, A. Sierakowski, W. Schaff, L. Eastman *et al.*, *J. Appl. Phys.* **87**, 334 (2000).

<sup>5</sup>R. Vetury, N. Q. Zhang, S. Keller, and U. K. Mishra, *IEEE Trans. Electron Devices* **48**, 560 (2001).

<sup>6</sup>G. Meneghesso, G. Verzellesi, R. Pierobon, F. Rampazzo, A. Chini, U. K. Mishra, C. Canali, and E. Zanoni, *IEEE Trans. Electron Devices* **51**, 1554 (2004).

<sup>7</sup>X.-H. Ma, J.-J. Zhu, X.-Y. Liao, T. Yue, W.-W. Chen, and Y. Hao, *Appl. Phys. Lett.* **103**, 033510 (2013).

<sup>8</sup>J. Joh and J. A. del Alamo, *IEEE Trans. Electron Devices* **58**, 132 (2011).

<sup>9</sup>S. Yang, C. Zhou, Q. Jiang, J. Lu, B. Huang, and K. J. Chen, *Appl. Phys. Lett.* **104**, 013504 (2014).

<sup>10</sup>W. Liao, Y. Chen, C. Chen, J. Chyi, and Y. Hsin, *Appl. Phys. Lett.* **104**, 033503 (2014).

<sup>11</sup>D. Bisi, M. Meneghini, F. A. Marino, D. Marcon, S. Stoffels, M. Van Hove, S. Decoutere, G. Meneghesso, and E. Zanoni, *IEEE Electron Device Lett.* **35**, 1004 (2014).

<sup>12</sup>M. Meneghini, D. Bisi, D. Marcon, S. Stoffels, M. Van Hove, T.-L. Wu, S. Decoutere, G. Meneghesso, and E. Zanoni, *Appl. Phys. Lett.* **104**, 143505 (2014).

<sup>13</sup>E. Bahat-Treidel, O. Hilt, R. Zhytnytska, A. Wentzel, C. Meliani, J. Wurfl, and G. Trankle, *IEEE Electron Device Lett.* **33**, 357 (2012).

<sup>14</sup>J.-G. Lee, B.-R. Park, C.-H. Cho, K.-S. Seo, and H.-Y. Cha, *IEEE Electron Device Lett.* **34**, 214 (2013).

<sup>15</sup>S. Lenci, J. Hu, M. Van Hove, N. Ronchi, and S. Decoutere, in *IEEE 26th International Symposium on Power Semiconductor Devices and IC's (ISPSD), 2014* (IEEE, 2014), pp. 265–268.

<sup>16</sup>S. Lenci, B. De Jaeger, L. Carbonell, J. Hu, G. Mannaert, D. Wellekens, S. You, B. Bakeroort, and S. Decoutere, *IEEE Electron Device Lett.* **34**, 1035 (2013).

<sup>17</sup>J. Hu, S. Stoffels, S. Lenci, N. Ronchi, R. Venegas, S. You, B. Bakeroort, G. Groeseneken, and S. Decoutere, *Microelectron. Reliab.* **54**, 2196 (2014).

<sup>18</sup>J. K. Kaushik, V. Balakrishnan, B. Panwar, and R. Muralidharan, *Semicond. Sci. Technol.* **28**, 015026 (2013).

<sup>19</sup>J. Hu, S. Lenci, S. Stoffels, B. D. Jaeger, G. Groeseneken, and S. Decoutere, *Phys. Status Solidi C* **11**, 862 (2014).

<sup>20</sup>D. K. Schroder, *Semiconductor Material and Device Characterization* (John Wiley & Sons, 2006).

<sup>21</sup>T. Okino, M. Ochiai, Y. Ohno, S. Kishimoto, K. Maezawa, and T. Mizutani, *IEEE Electron Device Lett.* **25**, 523 (2004).

<sup>22</sup>M. Tapajna, R. J. Simms, Y. Pei, U. K. Mishra, and M. Kuball, *IEEE Electron Device Lett.* **31**, 662 (2010).

<sup>23</sup>W. Lee, T. Huang, J. Guo, and M. Feng, *Appl. Phys. Lett.* **67**, 1721 (1995).